Numerical lifetime assessment of engine parts submitted to thermomechanical fatigue

Guy Lederer, Eric Charkaluk, Laetitia Verger, Andrei Constantinescu

Numerical Lifetime Assessment of Engine Parts Submitted to Thermomechanical Fatigue, Application to Exhaust Manifold Design

Guy Lederer, Eric Charkaluk and Laetitia Verger
PSA Peugeot-Citröen

Andrei Constantinescu
Ecole Polytechnique

ABSTRACT

In this work a numerical method for the design of components submitted to severe cyclic thermomechanical loading is developed. This tool is based on a Finite Element (FE) analysis. In a first part the temperature distribution is obtained and used in the second part for the mechanical computation. The analyses use the description of the geometry of the part, a precise information of the thermal properties, an appropriate behavior of the material at low and high temperature and a good assessment of the boundary conditions (heat transfer coefficients, contact, ...). This method is applied to asses the low cycle fatigue design of a diesel turbo-charged exhaust manifold in cast iron. These calculations, failure location and lifetime estimation, obtained on two versions of this component, are compared to experimental data. The results show a good agreement in terms of critical zones location and of lifetime comparison in both versions and permit thus to classify the versions.

INTRODUCTION

Computational fatigue design of engine parts submitted to thermomechanical loading includes a wide range of difficulties conducting to a complex problem. These difficulties stem from the precise identification of the thermal loading, the mechanical constitutive behavior which has to perform at both low and high temperatures and the fatigue criterion itself. Even if the previous points have extensively been studied in the last decades, one still lacks a global robust approach for lifetime assessment in an industrial design context. The constrains of the industrial are the matching of experimental results and numerical lifetime computations as well a project duration compatible with the ever shortening motor development schedules. Therefore one needs to concentrate in each step of the design method the complex physical phenomena in a series of simple models.

This paper focuses on the applications of computational mechanics on fatigue life assessment and presents the case study of an exhaust manifold. Therefore a series of intermediary results, such as material behavior or temperature distribution, is included as a part of the numerical method section.

CASE STUDY PRESENTATION

The presented method can be considered as a general approach for numerical lifetime prediction of parts under thermomechanical loading. In the sequel the example of an exhaust manifold has been chosen to illustrate this method.

ENGINE AND MANIFOLD DATA – Two prototype versions of a four cylinder 2.1 l turbocharged diesel engine have been studied both experimentally and numerically.

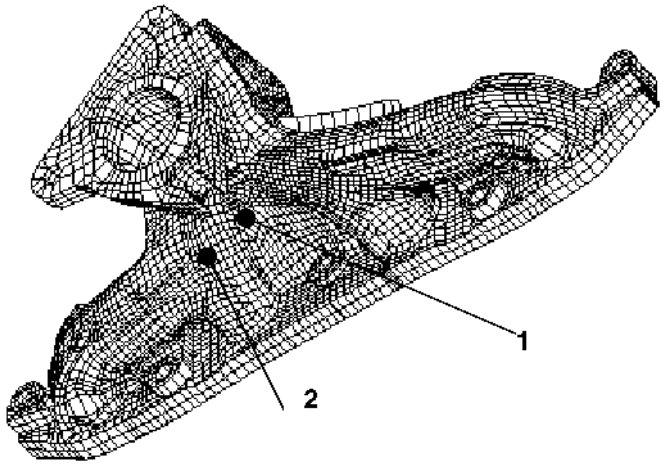

Figure 1. Exhaust manifold version 1

The mesh of version 1 of this manifold is presented figure 1. The second version (called version 2) differs only slightly from version 1 by typical modifications such as ribs or local thickness modifications (figure 11).

Both manifolds are made of a spheroidal graphite silicon/ molybdenum cast iron (4 wt% Si, 0.8 % Mo). The surface of the part has not been treated with the exception of the contact surfaces (cylinder head, screws, turbo) which been machined.

EXPERIMENTAL CONDITIONS – These two manifolds have been submitted to standard prototype durability cycles on a classical motor testing device. The test rig includes the whole motor, with its intake and exhaust ports, coupled with a controlled brake. The device is located in a ventilated room in order to keep a room temperature of 30°C, but with no special air blow system on the outer surface of the motor or the manifold. The cycle alternates continuously full load at 4000 rpm and light load at the same regime. The transient period from full to light load and light to full load takes 30s and the total cycle takes approximately 700 s. The external surface of the manifold is monitored by regular visual inspection and to detect crack apparition.

NUMERICAL METHOD

The numerical method will be presented here just in its global aspects without computational details.

The crucial points from the numerical point of view are:

- the sensitiveness of the result to the temperature distribution as it acts through the severe coupling with the mechanical material parameters determining the mechanical fields
- the choice of a mechanical constitutive law which has to represent the behavior at low and high temperatures and has to be identified from simple experiments
- the fatigue criterion which has to take into account the 3D nature of the mechanical fields and has to integrate these through an anisothermal cycle.

THERMAL COMPUTATION – The aim of the thermal computations is the prediction of the temperature field distribution on the manifold from engine data (i.e. exhaust gas temperature and mass flow rate) which can already be estimated in the early phases of the project.

The experimental cycle proposed here is a clearly transient one. However, in order to simplify the analysis we first determine a steady state temperature field distribution based on full load data and only afterwards compute the transient response under a series of assumptions concerning the evolution of the boundary conditions described are described in the *Transient temperature field* paragraph.

Steady-state temperature field – If the thermal conductivity is given as a function of temperature, the steady state diffusion problem can easily be solved provided that the boundary conditions are precisely evaluated. Three “families” of boundary conditions can be marked out: internal surface, external surface and contact conductance on contact surfaces.

1. Internal surface – The major heat flux contribution to the heating of the manifold comes from the forced convection with the exhaust gas. This is a tricky problem as the estimation of local convection coefficients needs a fair knowledge of both the fluid flow near the manifold wall and the gas temperature. The resolution of this fully turbulent anisothermal fluid problem is performed using the commercial FIRE code [1] and its description is out of the scope of this paper. However, let us simply summarize the assumptions at the basis of these computations :

- The mesh of the fluid part is generated automatically and the cell thickness in the wall neighborhood is adapted during the computations in order to get a correct evaluation of the boundary layer.
- The boundary conditions for the fluid computation are directly derived from engine and turbo-charger data, *i.e.* imposed gas temperature and fluid flow at the intake of the manifold and imposed pressure at the exhaust given by the turbocharger. The presented temperature distributions (see figures 2 and 3) are obtained under full load conditions.
- The anisothermal k-ε analysis does not show important differences in gas temperature between intake and exhaust for this kind of manifolds.
- The local heat transfer coefficient between the gas and the wall at full load has been obtained with the Diwakar law [2] based on a logarithmic description of the wall model. The resulting heat transfer coefficients at full load are then projected on the internal surface of the FEM mesh presented figure 1. The values of these coefficients can vary from approximately 200 W/m²°K to more than 1500 W/ m²°K near the turbocharger and depend on the local flow rate and the temperature of the gas.

2. External surface – The heat exchange on the external surface has been modeled using both natural convection with air at room temperature and radiation.

The natural convection coefficient *h* is derived from the classical empirical correlation [3]:

$$h = 0.53 \frac{R_a^{0.25} \lambda_f}{\phi_{ext}} \qquad (1)$$

where λ_f is the air conductivity at an estimated "film" temperature $T_f = \frac{T_p - T_{ext}}{2}$ (T_w and T_{ext} denoting

respectively the wall temperature of the manifold and the surrounding air temperature); ϕ_{ext} is a characteristic external diameter and R_a is the Rayleigh number evaluated at T_f . Equation (1) is valid for a laminar flow ($10^3 < R_a < 10^9$) and leads in our case to values of h typically around 20 W/m²°K.

The radiative part ϕ_r of the heat flow is simply computed by the classical radiation law:

$$\phi_r = \varpi(T)\beta(T^4 - T_{ext}^4) \quad (2)$$

where $\varpi(T)$ is the emissivity of the cast iron as a function of temperature and β is Stefan's constant. The radiant contribution to the heat flux is quite significant in hot zones of the manifold as $\varpi(T)$ reaches 0.9 for T_w around 700°C.

3. Contact surfaces – The thermal conduction between the manifold and the cylinder head or the turbo-charger is taken into account by means of a thermal contact conductance. For example the temperature field of the cylinder head in the vicinity of the manifold, T_{cyl}, being known from earlier analyses, the boundary condition, ϕ_{cont} , on the contact surface between cylinder head and manifold stands :

$$\phi_{cont} = \frac{1}{R_{Tc}}(T_w - T_{cyl}) \quad (3)$$

where T_w is as defined above and R_{Tc} denotes the contact resistance. This contact resistance integrates globally the thermal characteristics of the joint and of the interface. This parameter is obtained from measurements performed under representative clamping conditions.

FE computation – The conduction problem is solved using the ABAQUS Version 5.7 commercial FE code [4]. The convergence of this nonlinear problem takes some few iterations. The resulting temperature field is plotted figure 2. One can remark that the temperature exceeds 700°C near the turbo-charger and presents a spatial gradient of more than 400°C between the input and the output of the manifold (less than 0.2 m).

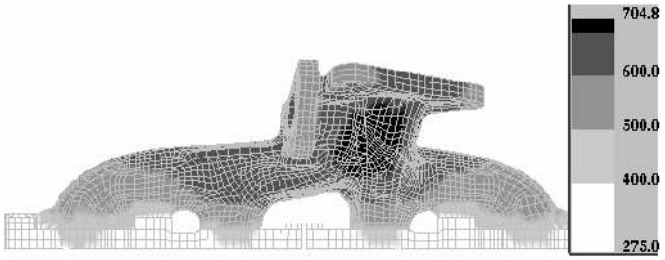

Figure 2. Steady-state temperature field at full load (°C)

Transient temperature field – Supposing that all boundary conditions are known at full load, the transient results are obtained under the following assumptions:

- At our time scale, the exchange temperature on the internal surface is directly dependent of the load evolution.
- The variation of convection coefficient on the internal surface between small and full load is neglected. This is due to the regime which remains slightly constant during the test and the assumption that, in first approximation, the convection coefficient follows this regime.
- The conduction coefficient on the external surface and contact conductance remain constant

The computations are performed using the transient analysis in ABAQUS/standard. The CPU time on a HP-V class computer is about 800s.

A comparison between the computed and measured temperature evolution is presented figure 3. The spatial location of the points quoted 1 and 2 is sketched on the manifold in figure 1. We can observe a good agreement between measured and computed temperature, even if the temperature rate reaches 15 °C/s.

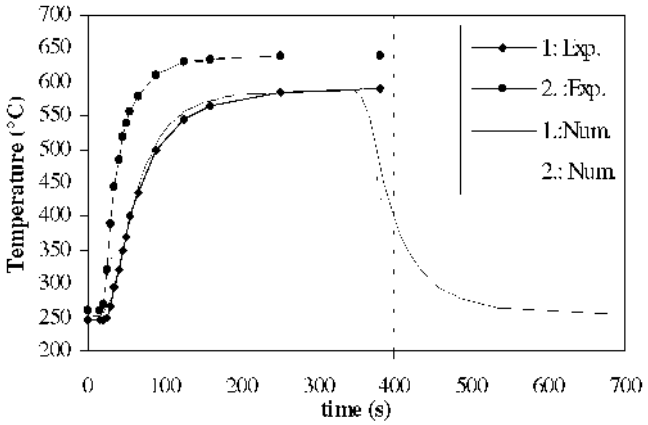

Figure 3. Steady-state temperature field at full load (°C). On this particular manifold, only the heating has been experimentally measured.

MATERIAL CHARACTERISTICS – The constitutive law has to characterize the material from 20 °C to 700 °C. At 20 °C it presents an elasto-plastic behavior and at 700 °C an almost purely viscous one. The fact that one has to deal with a simple unifying law over the whole temperature domain is dictated both by the FE transient analysis and the limited time devoted to the lifetime prediction during the development of a new manifold. This conducts to the choice of an elasto-visco-plastic material model. A similar conclusion has also been drawn by [5].

Elasto-Visco-Plastic (EVP) behavior – A reasonably representative model of the high temperature EVP behavior of the material is achieved with a viscoelastic-elastoplastic constitutive law with six temperature-depending parameters.

The stress state is described by the sum of two contributions of the elastoplastic part and the viscoelastic part of the model :

$$\boldsymbol{\sigma} = \boldsymbol{\sigma}_p + \boldsymbol{\sigma}_v = \mathbf{C}_p : \left(\boldsymbol{\varepsilon} - \boldsymbol{\varepsilon}_p\right) + \mathbf{C}_p : \left(\boldsymbol{\varepsilon} - \boldsymbol{\varepsilon}_p\right) \tag{4}$$

where C_p and C_v are the forth order tensors of the elastic moduli. The corresponding young moduli are denoted by K_p and K_v in the one-dimensional rheological representation of figure 4. ε_{vp} and ε_{vp} represent respectively the plastic and viscous strain tensor.

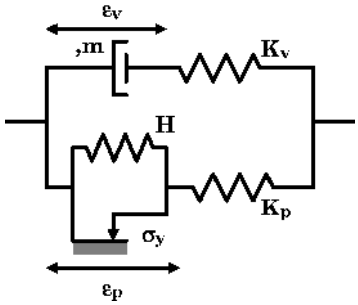

Figure 4. Rheological model for the cast iron

Both inelastic strains follow a flow rule described by a strain rate distance $\gamma \geq 0$ and a direction $\frac{\mathbf{A}}{\|\mathbf{A}\|}$ as $\dot{\boldsymbol{\varepsilon}}_{in} = \gamma \cdot \frac{\mathbf{A}}{\|\mathbf{A}\|}$.

The plastic law is given by a von Mises equivalent stress yield criterion J_2 and a linear kinematic hardening rule:

$$\begin{cases} \mathbf{A}_p = \mathbf{dev}\left(\boldsymbol{\sigma}_p\right) - \frac{2}{3} H.\boldsymbol{\varepsilon}_p \\ \gamma_p = \sqrt{\frac{3}{2}} \left\langle J_2\left(\mathbf{A}_p\right) - \boldsymbol{\sigma}_y \right\rangle \end{cases} \tag{5}$$

The viscous law is a three-dimensional Norton-Hoff rule :

$$\begin{cases} \mathbf{A}_v = \mathbf{dev}\left(\boldsymbol{\sigma}_v\right) \\ \gamma_v = \sqrt{\frac{3}{2}} \left\langle \frac{J_2\left(\mathbf{A}_v\right)}{\eta} \right\rangle^m \end{cases} \tag{6}$$

This model and its parameters have been identified from isothermal cyclic traction-relaxation tests at several temperatures. The parameters are then linearly interpolated between these identification temperatures. Figure 5 presents, for instance, the dependence of σ_y on temperature. One can remark that the yield limit lowers tremendously with increasing temperature and this will demand special care in the numerical integration algorithm.

Numerical implementation – The numerical implementation of this EVP law is performed in ABAQUS by means of a User Material (UMAT) [4]. This procedure allowed the optimization of both CPU time and robustness by use of a radial return algorithm [6-7] for the integration of the material behavior. This totally implicit implementation overcomes the difficulties of the standard « VISCO » analysis of ABAQUS which always tries an explicit algorithm before switching in implicit mode. Our algorithm is proved unconditionally stable whereas ABAQUS standard often presents slow convergence (leading to very little step sizes and high CPU costs) or even failure of convergence in severe transient loading conditions.

The numerical behavior of the material law has been tested on isothermal and anisothermal conditions before the complete manifold computation. The anisothermal computations correspond to a simple Thermo-Mechanical Fatigue specimen undergoing thermal cycles from 20 °C to 700 °C (the test is described later in the *fatigue life estimation* section). Computed temperatures and stresses have been compared with measured values and correlated satisfactorily.

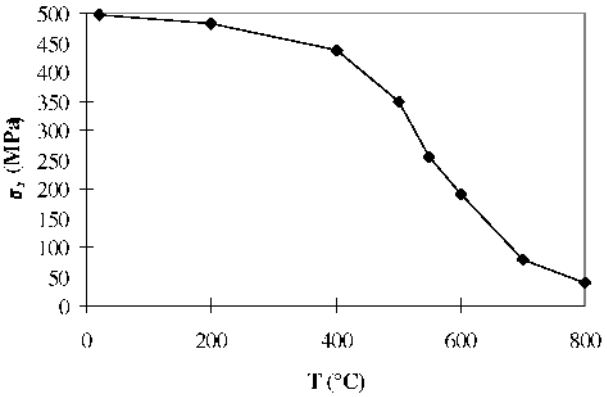

Figure 5. Evolution of the identified yield limit σ_y of the plastic part of the model

STRUCTURAL ANALYSIS – Finite Element Model and Boundary Conditions – The FE mesh of the manifolds contained about 15000 linear 3D brick elements, corresponding to about 66000 Degrees Of Freedom (DOF). The cylinder head has been modeled by a thick plate.

The coupling between the cylinder head and the manifold has been represented by a number of screws and a standard small sliding friction contact model [4].

Analysis – The analysis has been performed in two steps: first the manifold has been screwed on the cylinder head and second a series of thermal cycles have been computed. The imposed temperature distribution was a result of the previous presented transient analysis. The number of cycles has been chosen in order to obtain a stable limit cycle for the mechanical fields.

FATIGUE LIFE ESTIMATION – The major challenge was to determine a low cycle fatigue (LCF) criterion in a multiaxial context. The lifetime prediction of the parts should be included within the standard deviation of the experimental results. The experimental lifetime has been considered as the number of cycles to failure of a representative elementary volume. This approach also permits a separation of the structural aspects (multi-axial stress state, anisothermal loading, …) and the fatigue properties of the given material which can be established from simple classical laboratory LCF tests.

A close inspection of classical LCF laws shows that the Manson-Coffin [8-9], the Strain-Range Partitionning (SRP) [10] or the Smith-Watson-Topper (SWT) function [11] established in an isothermal and uniaxial context are not appropriate for this anisothermal problem. Two types of difficulties can be pointed out. The first one comes from the multiaxial aspect of our problem which makes difficult a generalization of these damage functions. The second one comes from the high range of attained temperatures: classical Manson-Coffin interpretation of isothermal LCF tests shows on a large difference in lifetime for the same plastic strain-range at different temperatures. This makes any interpretation of cumulated plastic strain on an anisothermal stress-strain curve hazardous.

Another difficulty can be remarked in the SWT interpretation of the anisothermal experiments as the choice of s_{max} is impossible in an anisothermal context $(\text{SWT function} = \sqrt{\text{E}.\sigma_{\max}.\Delta\varepsilon})$.

An interesting interpretation of the cyclic behavior of the material is presented by Skelton [12]. His results on LCF tests suggest that the cumulated dissipated energy to the plastic hardening or softening stabilization can be used as a crack initiation criterion in low cycle fatigue. Denoting by N_s the number of cycles to stabilization, assumed to correspond to crack initiation, Skelton showed that the cumulated dissipated energy to stabilization : $N_S \times \Delta W_S$ is relatively constant for a given material.

At this point, we shall assume that the failure of the representative elementary volume on real structures (which corresponds to N_f – number of cycles to failure - on specimen) conducts within a few cycles to a bad functioning of the structure in accordance with the fact that the engineering design should not guarantee the integrity of the component. Therefore, with both information – N_f and ΔW_s – a thermo-mechanical fatigue criterion can be established in the form : $N_f = f(\Delta W_S)$.

As a consequence of the previous considerations, the criterion has been established using classical isothermal LCF and anisothermal TMF tests [13-14]. The LCF tests have been carried out on classical specimens at different constant temperatures between 200°C and 700°C under strain control. The total strain rate was of 10^{-3} s^{-1} and the strain ranges were ± 0,25 %, ± 0,5 % and ± 1 % (R=-1). TMF tests were conducted on clamped specimens heated by the Joule effect. The tests are then in an out-of-phase mode. Maximum temperatures have been varied between 40°C and 700°C with an heating rate of 20°C/s. The maximum temperature has been obtained in a region of approximately 10 mm in the center of the specimen. The maximum temperature gradient was 30-40°C/mm. The parameters of the test are the clamp value (183000 N/mm and 227000 N/mm) and the dwell time at 700°C (60 seconds and 900 seconds).

For all tests the dissipated energy has been evaluated on the stabilized cycle by a numerical integration procedure from the stress-strain experimental curves for the LCF test and by FEM computations for the TMF tests. The experimental versus predicted lifetime is presented in log-log plot in Figure 6.

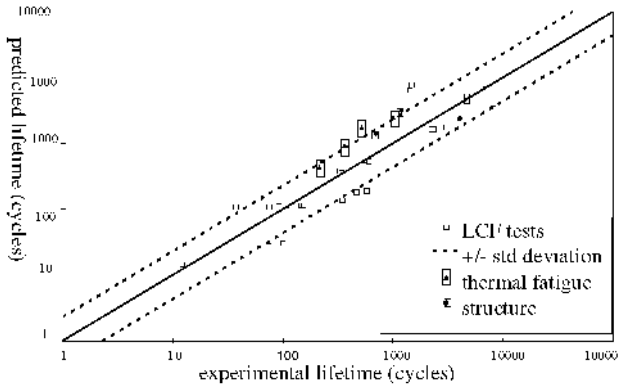

Figure 6. Experimental versus predicted lifetime for the nodular cast iron (structure : fatigue results on manifolds)

RESULTS

In the discussion of the result, we shall essentially present the predictions related to the two versions of the exhaust manifold. A detailed discussion of other results can be found in [7, 13-14].

NUMERICAL ASPECTS – The first remark concerns the number of cycles needed to achieve a stabilized limit cycle for the mechanical field, conducting to a stabilization of the cyclic dissipated energy. It appeared that three cycles were enough to get a representative value of the dissipated energy. Therefore, the next lifetime results are computed using the third loading cycle. It is important to notice that this is a pure observation and that to our knowledge no mathematical results are available to predict the existence of the limit cycle and the number of cycles needed to attain it.

The thermomechanical analyses for both manifold versions were completed within approximately 6 hours of CPU time on a HP-V class computer. This CPU time is only an indication since it is very sensitive to the amount

of inelastic deformations experienced by the structure as well as to the non-linearities induced by frictional contact.

FATIGUE RESULTS – Figure 7 presents a plot of the distribution of the criterion function on the inner surface of version 1.

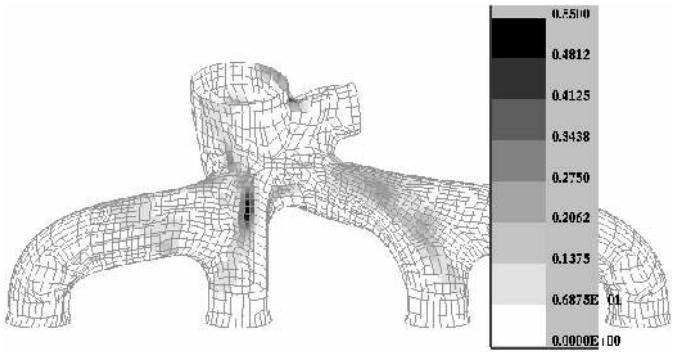

Figure 7. Version 1 ; main predicted crack zone ; visualized on the inner surface of the manifold

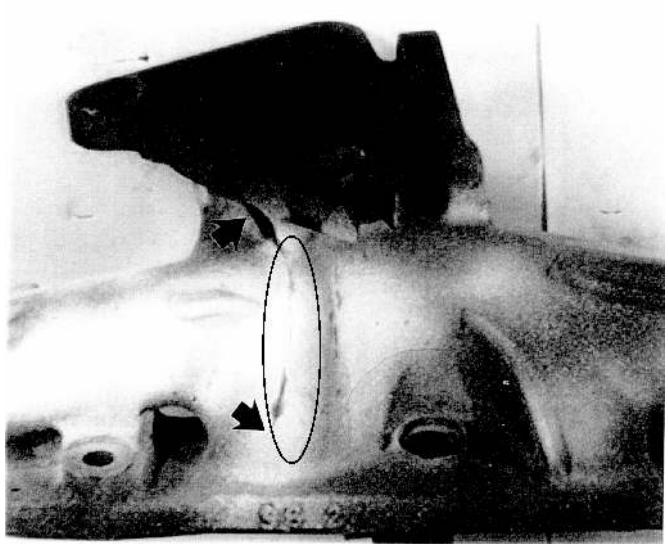

Figure 8. Version 1 ; first experimentally observed crack

The computed critical zone on the shortest tube of the manifold is in good agreement with one of the experimental cracked zone presented on figure 8.

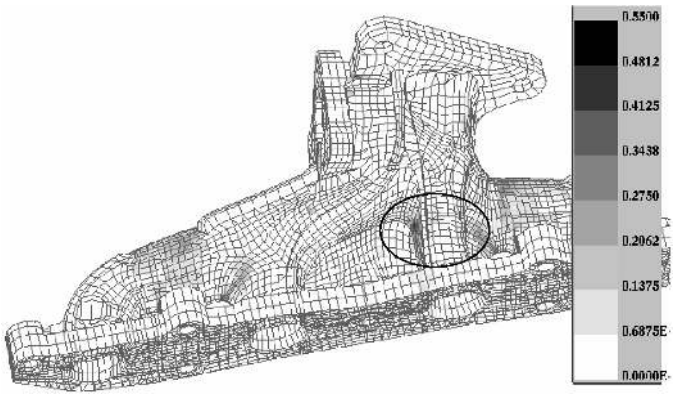

Figure 9. Version 1 ; second predicted crack zone at the back of the manifold

Figure 9 presents a second predicted zone on the rear of this version. The validity of this zone is also confirmed by experimental data as shown on figure 10. Both zones present approximately the same level of cracking danger, and the lifetime estimation falls within the standard deviation of the criterion as shown on figure 6 (points quoted « structure »).

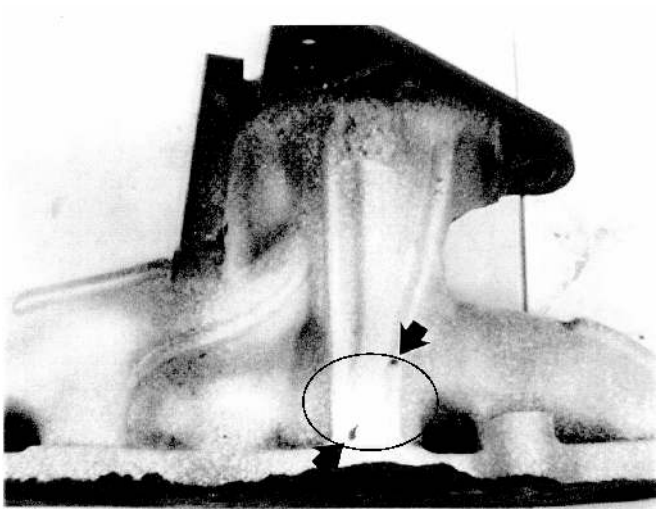

Figure 10. Version 1 ; second experimentally observed crack zone on the rear of the Manifold

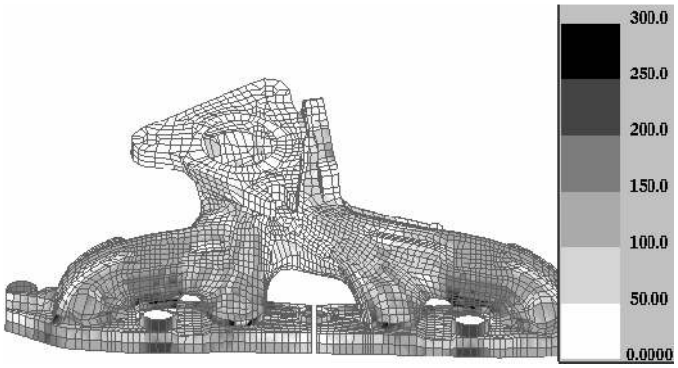

Figure 11. Version 2 ; Von Mises stress distribution (Mpa) at full load

Figure 11 presents an example of von Mises equivalent stress distribution at full load on version 2. It appears clearly that the highest von Mises equivalent stresses are located in the coldest parts of the manifold (see figure 2). This is coherent with the yield limit evolution sketched on figure 5, but gives no hint on the location of the critical zone.

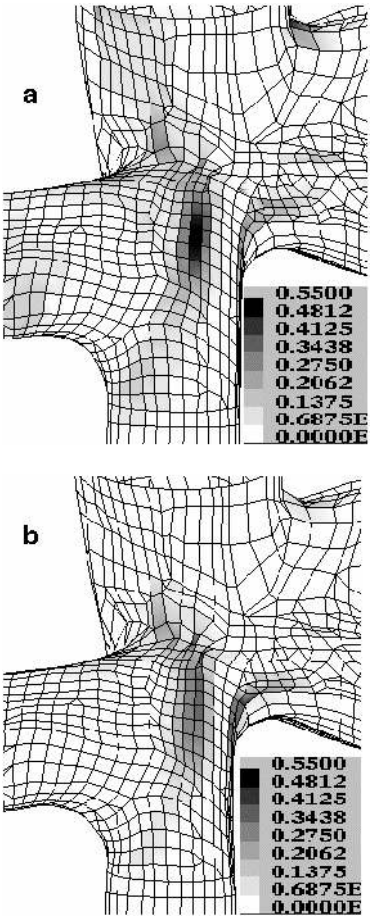

Figure 12. Criterion decrease (lifetime increase) between a, version 1 and b, version 2 for the first failure zone.

Computations performed on version 2 of this manifold exhibited an important increase in lifetime : The rear zone is not critical anymore, and the criterion shows a significant lifetime increase for the first zone, as detailed on figure 12. This predicted lifetime increase of 150% between version 1 and 2 can be satisfactorily compared with the experimental lifetime increase of 110%.

CONCLUSION

A complete lifetime estimation approach has been derived for structures undergoing thermomechanical fatigue. It has been applied to the design of cast iron exhaust manifolds.

The structural approach integrates a simple elasto-visco-plastic description of the high temperature behavior of the material. This material law allows sufficient precision without major CPU time increase implying that this approach can be included in a classical development schedule of such parts.

The results of these computations, associated with a reasonable simple anisothermal low cycle fatigue criterion show a good agreement between predicted and observed critical zones for two versions of a given manifold. Numerical and experimental lifetime increase between the two versions is also satisfactorily correlated.

This approach is not limited to exhaust manifolds or cast iron: further applications could concern steel or aluminum alloys and other parts in the automotive industry or elsewhere.

ACKNOWLEDGMENTS

The authors would like to thank Mr K. Dang Van, Ecole Polytechnique, and Mr A. Bignonnet, PSA Peugeot Citröen, for fruitfull discussion.

REFERENCES

1. AVL LIST GmbH, *FIRE Menu reference*, Graz (1996)
2. Taine J., Petit J.P., *Transferts thermiques et mécanique des fluides anisothermes,* Dunod, Paris (1989).
3. McAdams W.H, *Heat Transmission*, 3rd ed. Mc Graw Hill, (1954)
4. Hibbitt, Karlson & Soerensen Inc*, ABAQUS/Standard User's Manual*, (1998)
5. Anderson D. H., Bisaro D.R., Haan D.M., Olree M., SAE paper N° 980697, (1998).
6. Simo J.C. , Hughes T.J.R., *Computationnal Inelasticity*, Springer Verlag, (1998).
7. Charkaluk E., Verger L., Constantinescu A., Lederer G., Stolz C., in *Actes du 4ème Colloque de Calcul de Structure*, Teknea ed., Giens, (1999)
8. Coffin L. F, ASME paper 53-A76, pp 931-950, . (1953)
9. .Manson S., NACA TN 2933, . (1953).
10. .Halford, G. R., and Manson, S. , In : *Thermal fatigue of materials and components*, ASTM STP 612, pp 239-254, (1976).
11. Smith, K.N., Watson P. and Topper T. H., *J. Mater.* Vol. 5., No 4, pp 767-778, (1970).
12. Skelton R. P., *Mat. Sc. Tech.* Vol. 7, pp 427-439, (1991).
13. Charkaluk E., PhD Dissertation, Ecole Polythechnique, Palaiseau, France (1999).
14. Charkaluk E., Constantinescu A., Bignonnet A., Dang Van K., in *Low cycle fatigue and elasto-plastic behavior of materials* pp 119-130, K.T. Rie & R. D. Portella eds., Elsevier (1998).